DKK3 knockdown confers negative effects on the malignant potency of head and neck squamous cell carcinoma cells via the PI3K/Akt and MAPK signaling pathways

NAOKI KATASE[1,2], SHIN-ICHIRO NISHIMATSU[2,3], AKIRA YAMAUCHI[4], MASAHIRO YAMAMURA[5] and SHUICHI FUJITA[1]

[1]Department of Oral Pathology, Institute of Biomedical Sciences, Nagasaki University, Nagasaki, Nagasaki 852-8588; Departments of [2]Molecular and Developmental Biology, [3]Natural Sciences, [4]Biochemistry and [5]Clinical Oncology, Kawasaki Medical School, Kurashiki, Okayama 701-0192, Japan

Received May 16, 2018; Accepted October 12, 2018

DOI: 10.3892/ijo.2018.4667

Abstract. Dickkopf-related protein 3 (DKK3), which is a member of the Dickkopf WNT signaling pathway inhibitor family, is considered to be a tumor suppressor, due to its reduced expression in cancer cells and its ability to induce apoptosis when overexpressed by adenovirus. However, our previous study demonstrated alternative functions for DKK3 in head and neck squamous cell carcinoma (HNSCC). Our study reported that DKK3 expression was predominantly upregulated in HNSCC cell lines and tissue samples, and its expression was significantly correlated with poor prognosis. Furthermore, DKK3 overexpression in HNSCC cells significantly increased cancer cell proliferation, migration, invasion and *in vivo* tumor growth. These data have led to the hypothesis that DKK3 may exert oncogenic functions and may increase the malignant properties of HNSCC. The present study established a stable DKK3 knockdown cell line (HSC-3 shDKK3) using lentivirus-mediated short hairpin RNA, and assessed its effects on cancer cell behavior using MTT, migration and invasion assays. In addition, its effects on *in vivo* tumor growth were assessed using a xenograft model. Furthermore, the molecular mechanisms underlying the effects of DKK3 knockdown were investigated by microarray analysis, pathway analysis and western blotting. Compared with control cells, HSC-3 shDKK3 cells exhibited significantly reduced proliferation, migration and invasion, and formed significantly smaller tumor masses when subcutaneously transplanted into nude mice. In addition, in HSC-3 shDKK3 cells, the expression levels of phosphorylated (p)-protein kinase B (Akt) (Ser473), p-phosphoinositide 3-kinase (PI3K) p85 (Tyr467), p-PI3K p55 (Try199), p-3-phosphoinositide-dependent protein kinase-1 (PDK1) (Ser241) and total p38 mitogen-activated protein kinase (MAPK) were reduced. Furthermore, phosphorylation of mechanistic target of rapamycin (mTOR) (Ser2448) was slightly decreased in HSC-3 shDKK3 cells, which may be due to the increased expression of DEP domain-containing mTOR-interacting protein. Conversely, DKK3 overexpression in HSC-3 shDKK3 cells rescued cellular proliferation, migration and invasion. With regards to expression levels, p-PI3K and p-PDK1 expression was not altered, whereas mTOR and p-p38 MAPK expression was elevated. These data supported the hypothesis and indicated that DKK3 may contribute to the malignant phenotype of HNSCC cells via the PI3K/Akt/mTOR and MAPK signaling pathways.

Correspondence to: Dr Naoki Katase, Department of Oral Pathology, Institute of Biomedical Sciences, Nagasaki University, 1-7-1 Sakamoto, Nagasaki, Nagasaki 852-8588, Japan
E-mail: katase@nagasaki-u.ac.jp

Key words: head and neck squamous cell carcinoma, Dickkopf-related protein 3, phosphoinositide 3-kinase, protein kinase B, mitogen-activated protein kinase

Introduction

More than 90% of cases of head and neck cancer, including oral cancer, originate from the squamous epithelia; this type of cancer is referred to as head and neck squamous cell carcinoma (HNSCC). HNSCC is the sixth most common type of cancer, and a significant cause of cancer-associated mortality worldwide (1). The biological characteristics of HNSCC cells are highly diverse (2), and the molecular background that contributes to the heterogeneity of this cancer has yet to be elucidated, despite recent developments in molecular genetics. For the treatment of HNSCC, combined surgery, radiation and chemotherapy is often performed. However, particularly in cases with metastatic lesions, treatment is very complex, and the overall survival rate is poor. Therefore, the identification of key cancer-associated genes is required, which may contribute to the pathogenesis, progression and metastasis of HNSCC, and may be considered a therapeutic target.

As a specific cancer-associated gene candidate, our previous study led us to focus on the Dickkopf-related protein 3 (DKK3) gene, which is a member of the Dickkopf WNT signaling pathway inhibitor family. This protein family comprises

secreted proteins with two distinct cysteine-rich domains, which antagonize the Wnt ligand, thus functioning as negative regulators of oncogenic Wnt signaling (3). However, the DKK3 protein does not antagonize the Wnt protein; however, its constitutional function remains unclear. Previous studies have indicated that DKK3 possesses a tumor suppressor function; it has been reported that DKK3 expression is decreased in cancer (4,5), and that it may induce cancer cell apoptosis when overexpressed by adenovirus-mediated gene transfer (6,7).

Interestingly, the expression pattern and putative function of DKK3 in HNSCC differ from those in other types of cancer. Our previous study demonstrated that HNSCC tissue samples and cell lines predominantly express DKK3 gene and protein, and that its expression increases from low level in the cytoplasmic membrane to high cytoplasmic expression accompanied by progression of epithelial dysplasia, which is the precursor lesion of HNSCC (8). In addition, patients with HNSCC and high DKK3 protein expression exhibit significantly shorter disease-free survival and metastasis-free survival (9). Furthermore, small interfering RNA-mediated downregulation of DKK3 gene expression in HNSCC-derived cell lines results in significantly decreased cellular invasion and migration (10). Our previous study also demonstrated that DKK3 overexpression in a HNSCC cell line results in significantly elevated cellular proliferation, migration and invasion, as well as *in vivo* tumor growth, together with increased phosphorylation of protein kinase B (Akt) and cyclin D1 (CCND1), and c-myc mRNA expression (11). These results led to the hypothesis that DKK3 may specifically exert oncogenic functions in HNSCC.

The present study, using lentivirus-mediated short hairpin (sh)RNA, established a stable DKK3 knockdown cell line (HSC-3 shDKK3), and aimed to investigate the precise effects of DKK3 loss-of-function on HNSCC cells, and the detailed mechanism. Supporting our hypothesis, the results revealed that DKK3 knockdown reduced the malignancy of HNSCC cells.

Materials and methods

Cell lines. The human tongue cancer-derived cell line, HSC-3, was used in this study, which was purchased from RIKEN Bioresource Center (Tsukuba, Japan). Using this cell line as a parent cell line, stable DKK3 knockdown and control cell lines were generated [HSC-3 shDKK3 and HSC-3 scrambled shRNA (shScr), respectively]. The cell lines were maintained in Dulbecco's modified Eagle's medium (DMEM; Sigma-Aldrich; Merck KGaA, Darmstadt, Germany), supplemented with 10% fetal bovine serum (FBS; Nichirei Biosciences, Inc., Tokyo, Japan). For HSC-3 shDKK3 and HSC-3 shScr cells, 10 μg/μl puromycin (Wako Pure Chemical Industries, Ltd., Osaka, Japan) was additionally supplemented.

Generation of the HSC-3 shDKK3 cell line. For lentivirus-mediated shRNA targeting of DKK3, a DKK3 shRNA expressing vector [DKK3-Human, four unique 29mer shRNA constructs cloned into a lentiviral green fluorescent protein (GFP) vector; cat. no. TL313463; OriGene Technologies, Inc., Rockville, MD, USA] and a control vector (non-effective 29-mer shScr cassette cloned into a pGFP-C-shLenti Vector; cat. no. TR30021; OriGene Technologies, Inc.) were purchased and used according to the manufacturer's protocol. Briefly, $2.5x10^6$ 293T cells (RIKEN Bioresource Center) were seeded in a 100-mm dish in growth medium (DMEM supplemented with 10% FBS). The next day, 5 μg vectors containing shRNA constructs and 6 μg packaging plasmid (Lenti-vpak packaging kit; cat. no. TR30037; OriGene Technologies, Inc.) were transfected into the cells using MegaTran 1.0 (OriGene Technologies, Inc.); the cells were incubated at 37˚C in an atmosphere containing 5% CO_2 for 12 h. The supernatant containing viral particles was subsequently collected. HSC-3 cells were seeded in 12-well plate and the cells reached 60% confluence in 24 h. The next day, the medium was replaced with complete medium containing 8 μg/μl polybrene (Sigma-Aldrich; Merck KGaA) and 200 μl viral solution was added to the cells and incubated for 4 h at 37˚C in an atmosphere containing 5% CO_2. The cells were then cultivated in growth medium for 4 days. After passage into a 60-mm dish, the cells were incubated in growth medium supplemented with 10 μg/μl puromycin. The knockdown efficacy was confirmed by reverse transcription-quantitative polymerase chain reaction (RT-qPCR) and western blotting. The experimental protocol was approved by the Recombinant DNA Experiments Safety committee of Kawasaki Medical School (No. 13-14; Kurashiki, Japan).

RT-qPCR. Cells were cultured in 100-mm dishes or 6-well plates, and total RNA was extracted from cells using ISOGEN (Nippon Gene Co., Ltd., Tokyo, Japan) or Nucleospin RNA® (Macherey-Nagel GmbH, Düren, Germany). cDNA was synthesized using ReverTra Ace® (Toyobo Life Science, Osaka, Japan), according to the manufacturer's protocol. RT-qPCR was conducted using THUNDERBIRD® qPCR mix (Toyobo Life Science) on a StepOnePlus PCR system (Thermo Fisher Scientific, Inc., Waltham, MA, USA). Gene expression was quantified and normalized to the RPL30 housekeeping gene (12). The primer sequences were as follows: DKK3, forward 5'-CAGGCTTCACAGTCTGGTGCTTG-3', reverse 5'-ACATTGTTTCCATCTCCTCCCCTC-3'; RPL30, forward 5'-ACAGCATGCGGAAAATACTAC-3', reverse 5'-AAAGGAAAATTTTGCAGGTTT-3'; and CCND1, forward 5'-CTTCCTCTCCAAAATGCCAG-3' and reverse 5'-AGCGTGTGAGGCGGTAGTAG-3' (11). The PCR conditions were as follows: 95˚C for 1 min, followed by 40 cycles at 95˚C for 15 sec and 60˚C for 45 sec, and a final extension step at 95˚C for 15 sec. Absolute quantification was used for analyses as previously described (13).

Transfection of DKK3-expressing plasmid. An expression plasmid for full-length DKK3 was prepared in our previous experiment (11). HSC-3 cells were seeded at $1.5x10^6$ in a 100-mm dish, and the next day, 12 μg plasmids were transfected into the cells using Turbofectin 8.0™ (OriGene Technologies, Inc.) at 37˚C overnight in an atmosphere containing 5% CO_2. As a control for transfection, a $pCS2^+$ empty vector (Addgene, Cambridge, MA, USA) was used.

Western blotting. The cell lines (HSC-3, HSC-3 shScr and HSC-3 shDKK3) were maintained until they became 100% confluent. Subsequently, cells were lysed in immunoprecipitation buffer

[20 mM Tris-HCl (pH 8.0), 150 mM NaCl, 1 mM EDTA, 1% Triton X-100]. Protein concentration was quantified using the DC™ Protein Assay (Bio-Rad Laboratories, Inc., Hercules, CA, USA), and 10 μg protein was used for western blotting. Briefly, proteins were boiled in Laemmli's buffer for 3 min, loaded onto an e-PAGEL® precast gel (ATTO Corporation, Tokyo, Japan) and blotted onto polyvinylidene difluoride (PVDF) membranes. After blocking non-specific binding by soaking the PVDF membranes in PVDF Blocking Reagent for Can Get Signal® (Toyobo Life Science) at room temperature for 1 h, the membranes were incubated with primary antibodies at 4˚C overnight. The following primary antibodies were used in this study: DKK3 (1:10,000; cat. no. ab186409, Abcam, Cambridge, MA, USA), β-catenin (1:1,000; cat. no. 8480S), phosphorylated (p)-β-catenin (Ser675) (1:1,000; cat. no. 4176S), glycogen synthase kinase (GSK)-3β (1:1,000; cat. no. 12456S), p-GSK3β (Ser9) (1:1,000; cat. no. 5558S), transforming growth factor (TGF)-β (1:1,000; cat. no. 3711S), Akt (1:1,000; cat. no. 4685S), p-Akt (Ser473) (1:1,000; cat. no. 9271S), c-Jun (1:1,000; cat. no. 9165S), p-c-Jun (Ser63) (1:1,000; cat. no. 9261S), c-Jun N-terminal kinase (JNK) (1:1,000; cat. no. 9258S), p-JNK (Thr183/Tyr182) (1:1,000; cat. no. 9251S), phosphoinositide 3-kinase (PI3K) p110α (1:1,000; cat. no. 4249S), 3-phosphoinositide-dependent protein kinase-1 (PDK1) (1:1,000; cat. no. 5662S), p-PDK1 (Ser241) (1:1,000; cat. no. 3061S), mechanistic target of rapamycin (mTOR) (1:1,000; cat. no. 2972S), p-mTOR (Ser2448) (1:1,000; cat. no. 5536S), p38 MAPK (1:1,000; cat. no. 9212S), p-p38 MAPK (Thr180/Tyr182) (1:1,000; cat. no. 9211S), p44/p42 MAPK (1:1,000; cat. no. 9102S), p-p44/p42 MAPK (Thr202/Tyr182) (1:1,000; cat. no. 9101S), DEP domain-containing mTOR-interacting protein (DEPTOR) (1:1,000; cat. no. 11816S), β-actin (1:50,000; cat. no. 5057S) (Cell Signaling Technology, Inc. Danvers, MA, USA) and p-PI3K p85 (Y467)/p55 (Y199) (1:1,000; cat. no. BS4605; Bioworld Technology, Inc., St. Louis Park, MN, USA). Subsequently, the membranes were washed in Tris-buffered saline (TBS) containing 0.1% Tween-20, and were incubated with a secondary antibody (1:50,000; cat. no. 111-036-003; Jackson ImmunoReaserch Laboratories, Inc., West Grove, PA, USA) for 1 h at room temperature. Antibodies were diluted in Can Get Signal® (Toyobo Life Science). Proteins were visualized using the enhanced chemiluminescence prime western blotting detection system (GE Healthcare Life Sciences, Little Chalfont, UK).

Immunocytochemistry. Cells were fixed in PBS containing 4% paraformaldehyde for 10 min at room temperature. After three washes with PBS, cells were immunohistochemically stained with anti-DKK3 (1:200; cat. no. ab186409, Abcam) overnight at 4˚C. After washing, the cells were incubated with Alexa Fluor® 594-conjugated goat anti-rabbit secondary antibodies (1:500; cat. no. A11037; Thermo Fisher Scientific, Inc.) for 60 min at room temperature. Cell nuclei were stained with 1 μg/ml DAPI (cat. no. 342-07431; Dojindo Molecular Technologies, Inc., Kumamoto, Japan) for 60 min at room temperature. Fluorescent images were captured using a BZ-X710 All-in-One Fluorescence Microscope (Keyence Corporation, Osaka, Japan).

Cell proliferation assay. To assess the effects of DKK3 knockdown on cell proliferation, an MTT assay was performed using the TACS® Cell Proliferation Assay kit (Trevigen, Gaithersburg, MD, USA). HSC-3, HSC-3 shScr and HSC-3 shDKK3 cells were seeded into a 96-well microplate at $1.0x10^3$ cells/100 μl/well and were cultured for 24 h. MTT reagent was added to the cells and incubated for 4 h at 37˚C in an atmosphere containing 5% CO_2, resulting in the formation of formazan crystals. Subsequently, detergent agent included in the kit was added and absorbance was measured at 570 nm. Data were acquired on days 1, 3, 5 and 7.

Migration assay. The cell migration assay was performed using an Ibidi Culture-Insert (Ibidi GmbH, Munich, Germany). HSC-3, HSC-3 shScr and HSC-3 DKK3 cells were suspended in DMEM supplemented with 10% FBS ($1.0x10^6$ cells/ml); 70 μl cell suspension was transferred to each well of the Culture-Insert in a 6-well plate. After 24-h incubation at 37˚C in an atmosphere containing 5% CO_2, the Culture-Insert was removed using sterilized tweezers. Time-lapse photography was captured using a BZ-X700 microscope (Keyence Corporation). The area was measured using ImageJ software version 1.51 (http://rsb.info.nih.gov/ij/; National Institutes of Health, Bethesda, MD, USA).

Invasion assay. BioCoat™ Matrigel® Invasion Chambers (Corning Life Sciences, Bedford, MA, USA) were used to conduct an invasion assay, according to the manufacturer's protocol. Cells were harvested and suspended in serum-free DMEM at $2.5x10^5$ cells/ml; 500 μl cell suspension was added into the upper chambers. After 24-h incubation at 37˚C in an atmosphere containing 5% CO_2, the chambers were fixed and stained with Diff-Quik Stain™ (Lab Aids Pty Ltd., North Narrabeen, NSW, Australia) and mounted on a glass slide. Cell number was counted under an optical microscope (AxioSkop 2 plus; Carl Zeiss AG, Oberkochen, Germany) and relative cellular invasion (invasion index) was calculated according to the manufacturer's protocol.

Xenograft model and histological evaluation. Cells were suspended in PBS at $4.0x10^6$ cells/150 μl and were subcutaneously injected into the dorsal area of 5-week-old, male BALB/cAJcl-nu/nu nude mice (CLEA Japan, Inc., Tokyo, Japan). The animals had free access to food and water and were housed at 22˚C (60-70% humidity), under a 12-h light/dark cycle. The average body weight of the mice in each group was 22.70±0.34 g (HSC-3), 21.87±0.60 g (HSC-3 shScr) and 22.00±0.77 g (HSC-3shDKK3). A total of 30 mice were used in this study (n=10/experimental group), which were divided into three groups: i) Injected with HSC-3 cells, ii) injected with HSC-3 shScr, and iii) injected with HSC-3 shDKK3 cells. Tumor volume (V) was measured and calculated using the following formula: $V = 4/3\pi \times L/2 \times (W/2)^2$, where L, longest diameter and W, diameter perpendicular to L. A total of 4 weeks post-injection, the mice were sacrificed and tumors were collected for histological evaluation. This study was performed in accordance with the Guidelines for Animal Experiments at Kawasaki Medical School, and the animal protocol for this study was approved by the Animal Care and Use Committee of Kawasaki Medical School (no. 15-052, 2015). Tissues were then fixed in 10% neutral buffered formalin for 8 h at room temperature, embedded in paraffin, sectioned

at 4 μm and stained with hematoxylin-eosin (HE). For HE staining, 4-μm sections were stained with 0.1% hematoxylin at room temperature for 10 min. Following incubation with 1% hydrochloric acid in ethanol for 3 sec, the sections were stained with 0.5% eosin for 30 sec. In addition, tissues sections underwent immunohistochemistry (IHC) to detect Ki-67 (1:50; cat. no. M7240; Dako; Agilent Technologies, Inc., Santa Clara, CA, USA). Ki-67 positive cells were counted and Ki-67 labeling index was calculated. Briefly, antigen retrieval was conducted by heating the samples in Target Retrieval Solution, Citrate pH 6, (cat. no. S2369; Dako; Agilent Technologies, Inc.) using a pressure cooker for 15 min. IHC was performed using Vectastain *Elite* ABC Rabbit immunoglobulin G kit (cat. no. PK-6101; Vector Laboratories, Inc., Burlingame, CA, USA). Following antigen retrieval, the sections were incubated in methanol containing 0.3% H_2O_2 to block endogenous biotin for 30 min at room temperature. The sections were rinsed twice in TBS (5 min/rinse), and were then blocked with normal goat serum, from the kit, diluted in TBS (1:75) for 30 min at room temperature. The primary antibody was diluted in TBS (1:50) and the sections were incubated with it overnight at 4˚C. The secondary antibody, from the kit, was diluted in TBS and normal goat serum (TBS:normal serum:secondary antibody, 1:75:200), and the sections were incubated with it for 30 min at room temperature. After three washes in TBS (5 min/wash), the sections were incubated with avidin-biotin complex, from the kit, for 30 min at room temperature. Diaminobenzidine (cat. no. 343-00901; Dojindo Molecular Technologies, Inc.) was used to identify peroxidase activity. Finally, the sections were counterstained with Mayer's hemalum (cat. no. 109249; Merck KGaA) and were examined under an optical microscope (AxioSkop 2 plus; Carl Zeiss AG).

Microarray analysis and pathway analysis. Expression profiles were compared between HSC-3 and HSC-3 shDKK3 cells, and between HSC-3 shScr and HSC-3 shDKK3 cells. Labeling, hybridization, scanning and data processing were carried out using Toray 3D-Gene® (Human Oligo chip 25k, cat. no. TRT-XR126; Toray Industries, Inc., Tokyo, Japan), according to manufacturer's protocol. Minimum information about a microarray experiment (MIAME)-compliant array data, including raw data, were deposited in the Gene Expression Omnibus, National Center for Biotechnology Information with accession number GSE107403 (https://www.ncbi.nlm.nih.gov/geo/; currently private until November 30, 2018). Pathway analysis of the microarray data was performed using the Database for Annotation, Visualization and Integrated Discovery Bioinformatics Resources 6.8 (14,15).

Bioinformatics analysis of RNA expression data from The Cancer Genome Atlas (TCGA). TCGA dataset is a large cancer dataset that contains high-throughput sequencing data for protein-coding genes. In the present study, TCGA was used to investigate the association between DKK3 mRNA expression and overall survival. TCGA dataset was obtained from cBioPortal (http://www.cbioportal.org) (16,17) and The Human Protein Atlas (https://www.proteinatlas.org) (18). The data used for analyses were mRNA expression status of DKK3 in HNSCC [Head and Neck Squamous Cell Carcinoma (TCGA, Provisional), n=530], pancreatic cancer [Pancreatic Adenocarcinoma (TCGA, PanCancer Atlas), n=184], renal cancer [Kidney Renal Clear Cell Carcinoma (TCGA, Provisional), n=538 and Kidney Renal Papillary Cell Carcinoma (TCGA, Provisional), n=293] and prostate cancer [Prostate Adenocarcinoma (TCGA, PanCancer Atlas), n=494], and phosphatidylinositol-4,5-bisphosphate 3-kinase catalytic subunit α (PIK3CA), Akt1, β-catenin and DEPTOR in HNSCC. The fragments per kilobase of exon per million reads mapped (FPKM) units were used for mRNA expression amount, and the FPKM cut-off value was determined based on The Human Protein Atlas. Associations were analyzed using the Kaplan-Meier method with log-rank test. $P<0.05$ was considered to indicate a statistically significant difference.

Statistical analysis. All values are presented as the means ± standard deviation. Significant differences were determined using two-tailed Student's t-test with Bonferroni correction. All analyses were conducted using R version 3.5.1 (The R Foundation for Statistical Computing, Vienna, Austria; http://www.r-project.org/). $P<0.05$ was considered to indicate a statistically significant difference. All experiments were independently conducted at least three times.

Results

Evaluation of DKK3 knockdown by lentivirus-mediated shRNA in HSC-3 cells. The cells were maintained in DMEM with or without the selection pressure of puromycin. Subsequently, after the cells reached 100% confluence, mRNA and protein expression levels were detected by RT-qPCR and western blotting, respectively. As shown in Fig. 1A, the mRNA expression levels of DKK3 were significantly decreased in HSC-3 shDKK3 cells compared with in HSC-3 ($P<0.001$) and HSC-3 shScr ($P<0.001$) cells. There was no significant difference in DKK3 mRNA expression between the HSC-3 and HSC-3 shScr cells ($P=0.362$). Similarly, the protein expression levels of DKK3 were decreased in HSC-3sh DKK3 cells compared with in HSC-3 and HSC-3 shScr cells; however, there was no difference between HSC-3 and HSC-3 shScr cells (Fig. 1B). The results of immunocytochemistry were concordant with those of western blotting; the protein expression levels of DKK3 were decreased in HSC-3 shDKK3 cells (Fig. 1C).

DKK3 knockdown decreases cellular proliferation, migration and invasion in vitro. After confirming DKK3 knockdown, its effects on *in vitro* cellular proliferation, migration and invasion were determined. With regards to cellular proliferation, HSC-3 shDKK3 cells exhibited reduced proliferation, which was significant on day 3 (vs. HSC-3, $P<0.01$; vs. HSC-3 shScr, $P<0.001$), and sustained on day 5 (vs. HSC-3, $P=0.035$; vs. HSC-3 shScr, $P<0.001$) and day 7 (vs. HSC-3, $P=0.022$; vs. HSC-3 shScr, $P=0.015$). There was no significance detected between HSC-3 and HSC-3 shScr cells at any time point (day 3, $P=0.058$; day 5, $P=0.800$; day 7, $P=0.302$, respectively; Fig. 2A). Alongside decreased cellular proliferation, the mRNA expression levels of CCND1 were significantly decreased in HSC-3 shDKK3 cells (vs. HSC-3, $P<0.001$; vs. HSC-3 shScr, $P<0.001$), whereas there was no significance

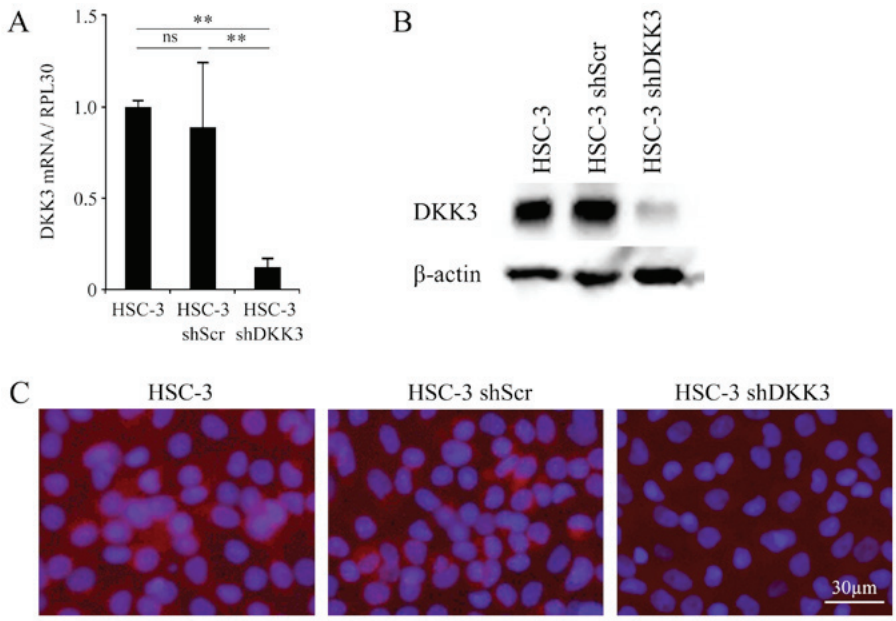

Figure 1. Lentivirus-mediated shRNA targeting DKK3 decreases DKK3 expression. (A) DKK3 mRNA expression was significantly decreased, as detected by reverse transcription-quantitative polymerase chain reaction. **P<0.01. (B) Western blotting and (C) immunocytochemistry indicated that DKK3 protein expression, which was observed in the cytoplasm, was decreased by shRNA. shScr did not affect DKK3 expression. Scale bar, 30 μm. DKK3, Dickkopf-related protein 3; ns, not significant; Scr, scrambled; sh/shRNA, short hairpin RNA.

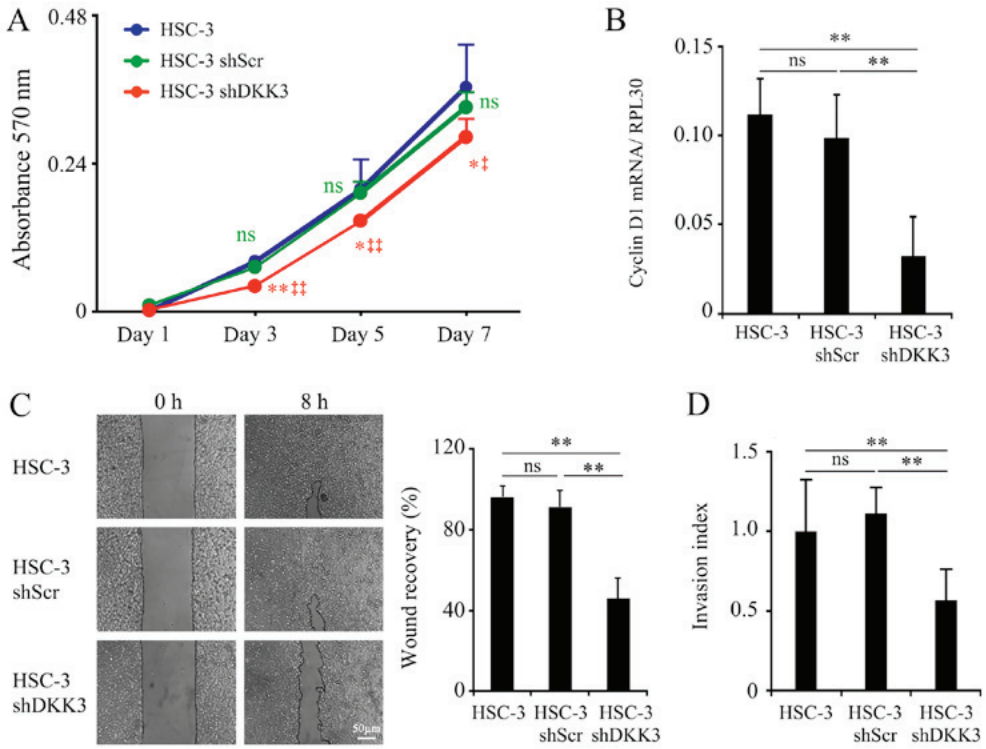

Figure 2. DKK3 knockdown by shRNA decreases proliferation, migration and invasion. (A) DKK3 knockdown decreased cellular proliferation. *P<0.05, **P<0.01 vs. HSC-3 cells; ‡P<0.05, ‡‡P<0.01 vs. HSC-3 shScr cells. (B) Cyclin D1 mRNA expression was significantly decreased in HSC-3 shScr cells. **P<0.01. (C) Cellular migration and (D) invasion were also significantly decreased in HSC-3 shDKK3 cells. Scale bar, 50 μm. **P<0.01. DKK3, Dickkopf-related protein 3; ns, not significant; Scr, scrambled; sh/shRNA, short hairpin RNA.

detected between HSC-3 and HSC-3 shScr cells (P=0.093; Fig. 2B).

Cellular migration was decreased in HSC-3 shDKK3 cells compared with in HSC-3 (P<0.001) and HSC-3 shScr cells (P<0.001), whereas there was no significance between HSC-3 and HSC-3 shScr cells (P=0.181; Fig. 2C). In addition, cellular invasion was diminished in HSC-3 shDKK3 cells (vs. HSC-3, P<0.001; vs. HSC-3 shScr, P<0.001). Conversely, HSC-3 shScr cells did not exhibit a significant difference compared with HSC-3 cells (P=0.112; Fig. 2D).

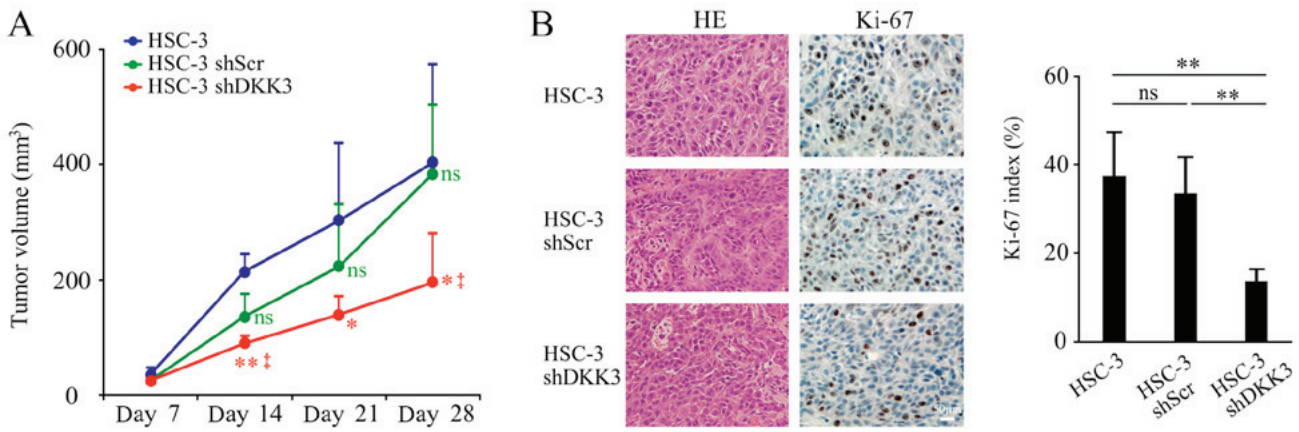

Figure 3. *In vivo* tumor growth, as assessed by a xenograft model. Cells were subcutaneously transplanted into nude mice. (A) Tumor volume formed by HSC-3 shDKK3 cells was significantly smaller than that of HSC-3 or HSC-3 shScr cells. *P<0.05, **P<0.01 vs. HSC-3 cells; ‡P<0.05 vs. HSC-3 shScr cells. (B) Ki-67 index revealed that tumor samples from the HSC-3 shDKK3 group exhibited reduced cell proliferation, compared with those from the HSC-3 or HSC-3 shScr groups. Scale bar, 50 μm. **P<0.01. DKK3, Dickkopf-related protein 3; HE, hematoxylin and eosin; ns, not significant; Scr, scrambled; sh/shRNA, short hairpin RNA.

DKK3 knockdown negatively affects in vivo tumor growth. To determine whether the *in vitro* results were replicable in *in vivo* experiments, HSC-3, HSC-3 shScr and HSC-3 shDKK3 cells were subcutaneously injected into nude mice. Tumor volume was observed from day 7 post-injection and gradually increased. On day 14 post-injection, tumor volume in the HSC-3 DKK3 group was significantly smaller than that in the HSC-3 (P=0.002) or HSC-3 shScr (P=0.022) groups. On day 21, tumor volume in the HSC-3 shDKK3 group was significantly smaller than that of HSC-3 cells (P=0.030), but was not significantly different when compared with HSC-s shScr cells (P=0.070). However, on day 28, the endpoint of the experiment, it was significantly smaller again (vs. HSC-3, P=0.021; vs. HSC-3 shScr, P=0.011, respectively). There was no significant difference between HSC-3 and HSC-3 shScr cells on any experimental day (day 7, P=0.146; day 14, P=0.055; day 21, P=0.459; day 28, P=0.814; Fig. 3A). After 28 days, the mice were sacrificed and tissues were collected for histological analyses. HE-stained sections exhibited no differences in cancer cell morphology or invasive behavior among the groups. The injected cells formed a local tumor mass, and did not exhibit distant or lymph node metastasis. The Ki-67 index was significantly lower in the HSC-3 shDKK3 group compared with in the HSC-3 (P=0.0017) and HSC-3 shScr (P=0.0012) groups, whereas there was no significance between the HSC-3 and HSC-3 shScr groups (P=0.514; Fig. 3B).

Microarray pathway analyses in DKK3 knockdown cells. Microarray analyses were performed to investigate gene expression alterations in HSC-3 shDKK3 cells. The results revealed that 2,026 and 2,029 genes were downregulated in HSC-3 shDKK3 cells, compared with in parental HSC-3 cells and HSC-3 shScr cells, respectively. Of these genes, 1,437 genes were commonly downregulated compared with in both HSC-3 and HSC-3 shScr cells. In addition, 862 and 2,925 genes were upregulated in HSC-3 shDKK3 cells, compared with in HSC-3 and HSC-3 shScr cells, respectively, of which 595 genes were commonly upregulated.

Pathway analyses were performed to determine the specific pathways, which may contribute to the reduced malignant properties in DKK3 knockdown cells. Firstly, the 1,437 commonly downregulated genes in HSC-3 shDKK3 cells were investigated, and 32 pathways were obtained, including 'RNA transport', 'Ribosome biogenesis in eukaryotes', 'Cell cycle', 'Endocytosis', 'p53 signaling pathway', 'Hepatitis B', 'Bladder cancer', 'Viral carcinogenesis', 'Colorectal cancer' and 'RIG-I-Like receptor signaling pathway', etc. The genes associated with these pathways are listed in Table I.

As for upregulated genes, pathway analysis of the 595 genes revealed 18 pathways. The majority of the upregulated genes in HSC-3 shDKK3 cells were involved in metabolic pathways, and did not include genes which are thought to be important to cancer proliferation, migration and invasion (data not shown). Therefore, this study focused on the pathways associated with the commonly downregulated genes. The downregulated genes included some important genes, including those involved in the PI3K/mTOR/Akt pathway (phosphoinositide-3-kinase regulatory subunit 1), MAPKs (MSPK8, MAPK kinase-4, MAPK kinase kinase-7 and MAPK kinase kinase kinase-3), cell cycle-associated genes (CCND1, cyclin E2 and cyclin-dependent kinase-1), chemokines [C-X-C motif chemokine ligand 8 (CXCL8)] and oncogenes (KRAS proto-oncogene, GTPase, BMI1 proto-oncogene, polycomb ring finger, MYB proto-oncogene like 1, SKI like proto-oncogene).

Based on these data, the present study investigated the PI3K/mTOR/Akt, MAPK and Wnt signaling pathways using western blotting, since these pathways are thought to be closely associated with HNSCC proliferation, migration and invasion, or DKK/Wnt signaling.

DKK3 knockdown affects signaling pathways. To identify the signaling pathways in which alterations in DKK3 expression are involved western blotting was performed. Proteins associated with the Wnt/β-catenin, PI3K/mTOR/Akt and MAPK pathways, including JNK were detected. These signaling pathways were chosen based on our previous study, which revealed that DKK3 overexpression in HNSCC cells elevates phosphorylation of Akt and c-Jun (12). The results revealed that DKK3 knockdown did not affect phosphorylation

Table I. Pathways associated with the downregulated genes in HSC-3 shDKK3 cells.

Term	Genes	P-value
RNA transport	FXR1, NMD3, RANBP2, THOC2, UPF2, UPF3A, UPF3B, EIF1AY, EIF2S2, EIF5B, XPO1, XPOT, FMR1, MAGOHB, NXT2, NUP153, NUP35, NUP54, PHAX, PNN, RPP40, SUMO1, TPR	$4.00x10^{-5}$
Ribosome biogenesis in eukaryotes	XRN1, FCF1, GNL2, GNL3, MPHOSPH10, NMD3, NOP58, RIOK2, WDR43, WDR75, AK6, EFL1, XPO1, NXT2, RPP40	$9.00x10^{-5}$
Protein processing in endoplasmic reticulum	BAG2, DNAJA1, DNAJB11, DNAJC10, DNAJC3, EDEM3, NGLY1, SEC24A, SEC63, UGGT2, YOD1, ATF6B, ERO1B, HSP90AA1, HSPA1A, MAN1A2, MBTPS2, MAPK8, NFE2L2, PLAA, UBE2D1	$2.70x10^{-4}$
RIG-I-like receptor signaling pathway	CXCL8, DDX3X, DDX58, TBK1, TANK, ATG12, ATG5, CHUK, IFNE, MAPK8, MAP3K7, SIKE1	$6.20x10^{-4}$
Hepatitis B	CXCL8, DDX3X, DDX58, E2F3, FAS, KRAS, RB1, TBK1, ATF6B, CASP3, CHUK, CCND1, CCNE2, MAPK8, MAP2K4, PIK3R1, TLR3, TGFBR1	$8.40x10^{-4}$
Endocytosis	ARFGEF1, ARAP2, ASAP1, ASAP2, ACAP2, KIAA1033, RAB11FIP2, RAB5A, SMURF2, VPS26A, WWP1, CAPZA1, CAPZA2, CHMP4C, EEA1, HSPA1A, KIF5B, PRKCI, RABEP1, SNX2, SNX4, SPG20, TGFBR1, USP8, VPS36, VTA1, ZFYVE16	$1.00x10^{-3}$
Fanconi anemia pathway	ATR, BRIP1, BRCA2. POLI, POLK, FANCB, FANCM, REV3L, RMI1, USP1 FANCM, REV3L, RMI1, USP1	$1.10x10^{-3}$
Pathways in cancer	APC, BRCA2, CXCL8, E2F3, FAS, KRAS, RB1, ROCK1, ROCK2, SOS2, BIRC2, BIRC3, CASP3, CCDC6, CHUK, CUL2, CC-ND1, CCNE2, FZD3, FZD6, HSP90AA1, HDAC2, HIF1A, ITGA2, ITGB1, LAMA3, LPAR1, LPAR6, MAPK8, MSH2, PIK3R1, PTGS2, PRKACB, TGFBR1, TPR	$1.10x10^{-3}$
NOD-like receptor signaling pathway	CXCL8, SUGT1, BIRC2, BIRC3, CHUK, ERBIN, HSP90AA1, MAPK8, MAP3K7, RIPK2	$1.40x10^{-3}$
Signaling pathways regulating pluripotency of stem cells	APC, BMI1, JAK2, KRAS, KLF4, SKIL, SMARCAD1, BMPR1A, FZD3, FZS6, INHBA, IL6ST, PIK3R1, PCGF5, PCGF6, RIF1, ZFHX3	$1.60x10^{-3}$
Spliceosome	DDX42, DDX46, RBM25, THOC2, U2SURP, CRNKL1, HSPA1A, HNRNPA3, MAGOHB, PLRG1, PRPF18, PRPF38B, PRPF40A, SRSF10, SRSF5, SF3B1	$2.50x10^{-3}$
Small cell lung cancer	E2F3, RB1, BIRC2, BIRC3, CHUK, CCND1, CCNE2, ITGA2, ITGB1, LAMA3, RIK3R1, PTGS2	$3.20x10^{-3}$
mRNA surveillance pathway	HBS1L, PCF11, RNMT, UPF2, UPF3A, UPF3B, CPSF2, MAGOHB, NXT2, PNN, PAPOLA, PPP1CC	$5.40x10^{-3}$
Pancreatic cancer	BRCA2, E2F3, KRAS, RB1, CHUK, CCND1, MAPK8, RIK3R1, TGFBR1	$1.50x10^{-2}$
Non-homologous end-joining	LIG4, MRE11, RAD50, XRCC4	$2.40x10^{-2}$
Chronic myeloid leukemia	E2F3, KRAS, RB1, SOS2, CHUK, CCND1, HDAC2, PIK3R1, TGFBR1	$2.60x10^{-2}$
Colorectal cancer	APC, KRAS, CASP3. CCND1, MAPK8, MSH2, PIK3R1, TGFBR1	$3.40x10^{-2}$
TNF signaling pathway	FAS, ATF6B, BIRC2, BIRC3, CASP3, CHUK, MAPK8, MAP2K4, MAP3K7, PIK3R1, PTGS2	$3.80x10^{-2}$
Shigellosis	CXCL8, ROCK1, ROCK2, ATG5, CHUK, ITGB1, MAPK8, RIPK2	$3.90x10^{-2}$
Proteoglycans in cancer	FAS, KRAS, ROCK1, ROCK2, SOS2, CASP3, CCND1, FZD3, FZD6, HIF1A, ITGA2, ITGB1, PIK3R1, PRKACB, PPP1CC, RDX, RPS6KB1	$4.10x10^{-2}$
Cell cycle	ATR, E2F3, RB1, TTK, CCND1, CCNE2, CCNH, CDK1, HDAC2, ORC3, STAG2, SMC3	$4.50x10^{-2}$
p53 signaling pathway	ATR, FAS, CASP3, CCND1, CCNE2, CDK1, PMAIP1, ZMAT3	$4.90x10^{-2}$
Epithelial cell signaling in *Helicobacter pylori* infection	ADAM10, ADAM17, ATP6V1C1, CXCL8, CASP3, CHUK, MAPK8, MAP2K4	$4.90x1^{0-2}$
Epstein-Barr virus infection	CD58, DDX58, RB1, TBK1, CHUK, CDK1, XPO1, HSPA1A, HDAC2, MAPK8, MAP2K4, MAP3K7, PIK3R1, PSMC6, PRKACB, RBPJ	$5.20x10^{-2}$

Table I. Continued.

Term	Genes	P-value
MAPK signaling pathway	FAS, KRAS, RASA1, RAPGEF2, SOS2, TAOK1, CASP3, CHUK, HSPA1A, IL1A, LAMTOR3, MAPK8, MAP2K4, MAP3K2, MAP3K7, MAP4K3, PRKACB, RPS6KA3, STK3, TGFBR1	$5.20x10^{-2}$
Homologous recombination	BRCA2, MRE11, RAD50, RAD54B, NBN$5.40x10^{-2}$	
Toxoplasmosis	JAK2, BIRC2, BIRC3, CASP3, CHUK, HSPA1A, ITGB1, LAMA3, MAPK8, MAP3K7, PIK3R1	$7.00x10^{-2}$
Prostate cancer	E2F3, KRAS, RB1, SOS2, CHUK, CCND1, CCNE2, HSP90AA1, PIK3R1	$7.20x10^{-2}$
Herpes simplex infection	DDX58, FAS, JAK2, SP100, TBK1, CASP3, C5, CHUK, CDK1, HCFC2, MAPK8, MAP3K7, PPP1CC, SRSF5, TLR3	$7.30x10^{-2}$
HTLV-I infection	APC, ATR, E2F3, ETS1, KRAS, MYBL1, RB1, ATF1, CHUK, CCND1, DLG1, XPO1, FZD3, FZD6, MAP2K4, NFYB, PI3KR1, PRKACB, TGFBR1	$8.80x1^{0-2}$
Viral carcinogenesis	DDX3X, KRAS, RB1, SP100, ATF6B, CASP3, CCND1, CCNE2, CDK1, DLG1, HDAC2, IL6ST, PMAIP1, PIK3R1, PRKACB, RBPJ	$8.80x10^{-2}$
Influenza A	CXCL8, DDX58, DNAJC3, FAS, JAK2, TBK1, XPO1, HSPA1A, IL1A, MAPK8, MAP2K4, NXT2, PIK3R1, TLR3	$9.40x10^{-2}$

shDKK3, Dickkopf-related protein 3 short hairpin RNA.

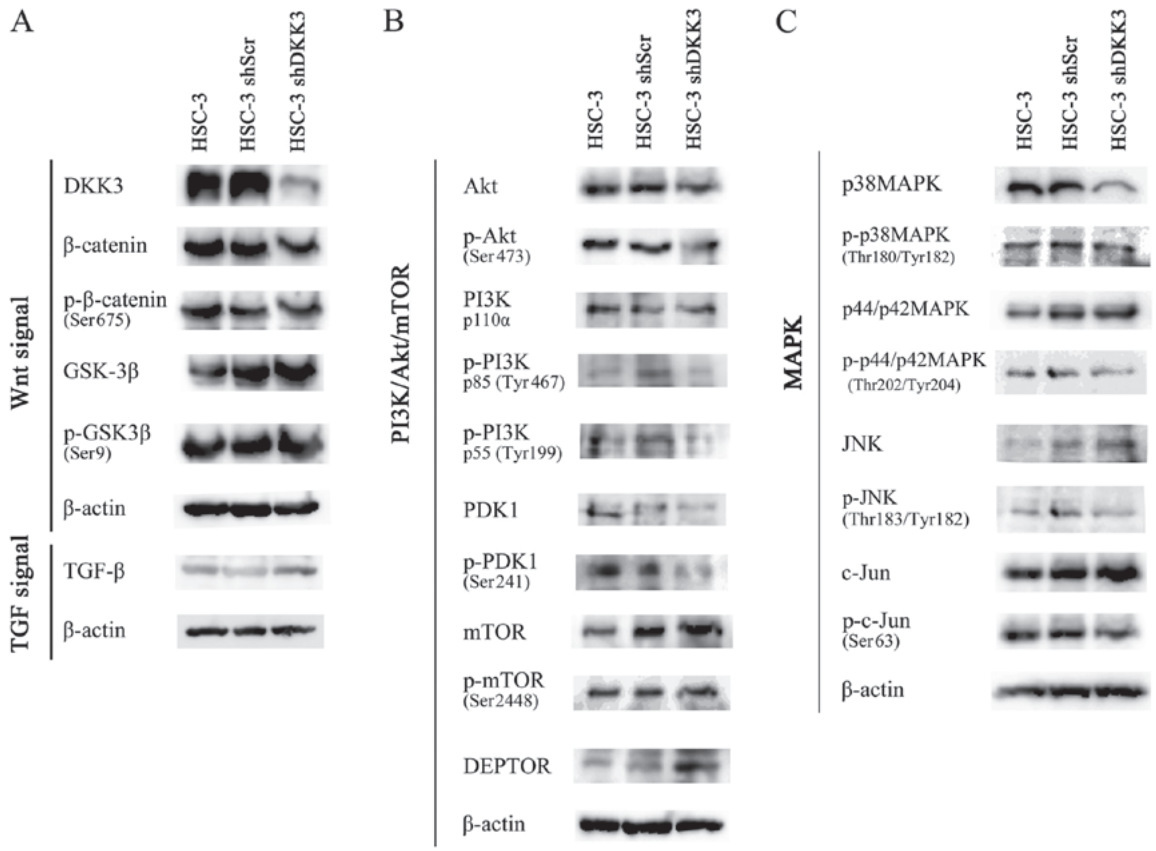

Figure 4. Western blotting revealed alterations in protein expression and phosphorylation status. (A) DKK3 knockdown did not affect phosphorylation of β-catenin (Ser675) or GSK-3β (Ser9). (B and C) Phosphorylation of Akt (Ser473) was decreased, together with the expression of p-PI3K p85 (Tyr467), p-PI3K p55 (Tyr199), p-PDK1 (Ser241), p38 MAPK and p-p38 MAPK (Thr180/Tyr182), in HSC-3 shDKK3 cells. (B) DEPTOR expression was increased, and phosphorylation of mTOR (Ser2448) was decreased in HSC-3 shDKK3 cells. (C) c-Jun (Ser63) or p-JNK (Thr183/Tyr182) expression was not altered. Akt, protein kinase B; DEPTOR, DEP domain-containing mTOR-interacting protein; DKK3, Dickkopf-related protein 3; GSK-3β, glycogen synthase kinase-3β; JNK, c-Jun N-terminal kinase; MAPK, mitogen-activated protein kinase; mTOR, mechanistic target of rapamycin; p, phosphorylated; PDK1, phosphoinositide 3-kinase; PI3K, phosphoinositide 3-kinase; Scr, scrambled; sh/shRNA, short hairpin RNA; TGF-β, transforming growth factor-β.

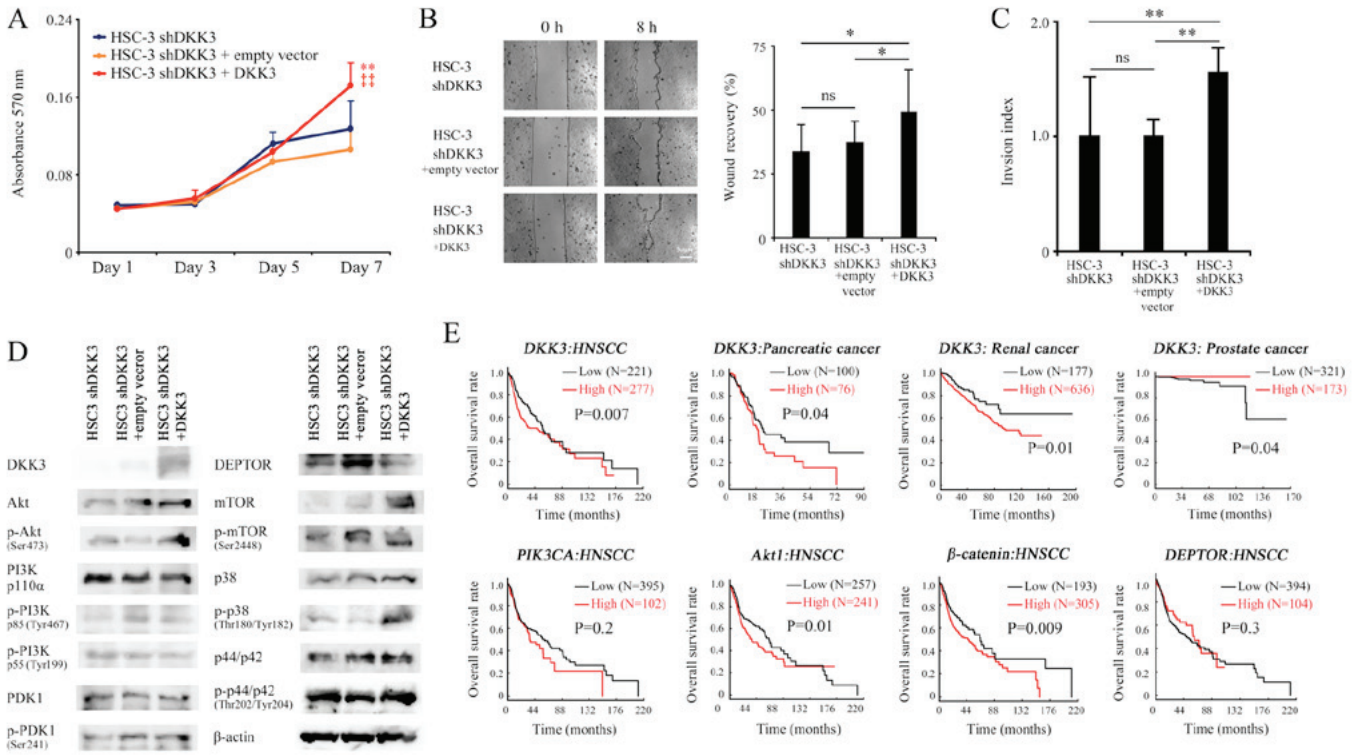

Figure 5. Effects of transfection with a DKK3-expressing plasmid on HSC-3 shDKK3 cells. (A-C) DKK3 overexpression significantly rescued cellular proliferation, migration and invasion, (D) elevated phosphorylation of Akt (Ser473) and p38 mitogen-activated protein kinase (Thr180/Tyr204), and decreased expression of DEPTOR. Scale bar, 50 μm. *P<0.05, **P<0.01 vs. HSC-3 cells; ‡‡P<0.01 vs. HSC-3 shScr cells. (E) Kaplan-Meier analyses based on The Cancer Genome Atlas database revealed that high DKK3 expression was associated with poorer OS in HNSCC, pancreatic cancer and renal cancer, whereas, in prostate cancer, high DKK3 expression was associated with a better OS. Although not significant, the data revealed that high mRNA expression levels of PIK3CA and low mRNA expression levels of DEPTOR may be attributed to a poorer OS, whereas high mRNA expression levels of Akt1 and β-catenin were significantly associated with poorer prognosis. Akt, protein kinase B; DEPTOR, DEP domain-containing mTOR-interacting protein; DKK3, Dickkopf-related protein 3; HNSCC, head and neck squamous cell carcinoma; mTOR, mechanistic target of rapamycin; ns, not significant; OS, overall survival; p, phosphorylated; PDK1, phosphoinositide 3-kinase; PI3K, phosphoinositide 3-kinase; PIK3CA, phosphatidylinositol-4,5-bisphosphate 3-kinase catalytic subunit α; Scr, scrambled; sh/shRNA, short hairpin RNA.

of β-catenin (Ser675) or GSK-3β (Ser9), thus suggesting that DKK3 might not function via the Wnt/β-catenin pathway in HNSCC cells. In addition, DKK3 knockdown resulted in only a slight alteration in TGF-β expression (Fig. 4A).

Corresponding to our previous data, the results revealed that phosphorylation of Akt (Ser473) was decreased in HSC-3 shDKK3 cells, which may be due to the decreased phosphorylation of PI3K and PDK1. Intriguingly, phosphorylation of mTOR (Ser2448) was slightly decreased, whereas the expression of DEPTOR was increased, which is a structural element of the mTOR complex (mTORC) that functions as a negative regulator of mTORC (Fig. 4B). The expression levels of p38 MAPK were markedly decreased in HSC-3 shDKK3 cells, and phosphorylation of c-Jun (Ser63) and p38 MAPK (Thr180/Tyr182) were slightly decreased in HSC-3 shDKK3 cells (Fig. 4C). The slight decrease in p-p38MAPK (Thr180/Tyr182) may be affected by the decreased expression of total p38 MAPK. From these results, it was hypothesized that DKK3 may stimulate certain cell surface receptors and drive PI3K/Akt/mTOR and MAPK signaling pathways, and/or facilitate DEPTOR degradation and activate Akt via mTOR.

DKK3 overexpression in HSC-3 shDKK3 cells. A DKK3-expressing plasmid was transfected into HSC-3 shDKK3 cells and its effects were assessed, in order to confirm whether exogenous overexpression of DKK3 cancels the negative effects of DKK3 knockdown on the malignant properties of cancer cells. Transfection with the plasmid successfully elevated DKK3 expression and significantly increased cancer cell proliferation on day 7 (vs. HSC-3 shDKK3, P=0.004; vs. HSC-3 shDKK3 + empty vector, P<0.001), migration (vs. HSC-3 shDKK3, P=0.010; vs. HSC-3 shDKK3 + empty vector, P=0.037) and invasion (vs. HSC-3 shDKK3, P<0.001; vs. HSC-3 shDKK3 + empty vector, P<0.001). Conversely, the empty vector did not affect proliferation on day 7 (P=0.095), migration (P=0.352) or invasion (P=0.063) compared with the HSC-3 shDKK3 group (Fig. 5A-D).

Western blotting revealed that DKK3 overexpression in HSC-3 shDKK3 cells rescued the expression of DKK3, and elevated phosphorylation of Akt (Ser473) and p38 MAPK (Thr180/Tyr204). In addition, DKK3 overexpression decreased DEPTOR and, in turn, increased expression of mTOR. However, phosphorylation of PI3K and PDK1 was not altered in response to DKK3 overexpression (Fig. 5D).

Association between DKK3 and PI3K/Akt/mTOR signaling molecules, and cancer prognosis. To evaluate whether DKK3 expression serves a prognostic role in cancer, the mRNA expression levels of DKK3 were analyzed in HNSCC, pancreatic cancer, renal cancer and prostate cancer using

TCGA data. The results revealed that high DKK3 expression was associated with poorer overall survival (OS) in HNSCC, pancreatic cancer and renal cancer; however, in prostate cancer, high DKK3 expression was associated with a better OS.

The present study also associated the association between PI3K/Akt/mTOR signaling molecules and HNSCC. Although not significant, the data revealed that high mRNA expression levels of PIK3CA and low mRNA expression levels of DEPTOR may be attributed to a poorer OS. Importantly, high mRNA expression levels of Akt1 and β-catenin were significantly associated with poorer prognosis (Fig. 5E).

Discussion

HNSCC is common malignancy worldwide, which is characterized by highly diverse biological behavior. It is widely accepted that HNSCC occurs as a result of cumulative genetic/epigenetic abnormalities in cancer-associated genes. However, to date, a limited number of genes have been reported as candidate somatic drivers for HNSCC, including tumor protein p53 (19), Akt1, APC, CCND1, fibroblast growth factor receptor 3 (FGFR3), NOTCH1, phosphatidylinositol-4,5-bisphosphate 3-kinase catalytic subunit alpha (PI3KCA), and phosphatase and tensin homolog (PTEN) (20-24). In addition, the HNSCC-specific cancer-associated genes/pathways are not well illustrated.

We previously aimed to detect specific HNSCC- associated genes by genome wide loss of heterozygosity analyses (25,26), and focused on DKK3. DKK family members can bind to lipoprotein receptor-related protein 5/6 (LRP5/6), by the β-propeller domain via a cysteine rich domain (C2), and negatively regulate oncogenic Wnt signaling (27). However, due to the differences in amino acid sequences in C2, DKK3 cannot bind to LRP5/6 (28); therefore, DKK3 is not thought to modulate oncogenic Wnt signaling.

Our previous studies have illustrated unique and specific expression of DKK3 in HNSCC (8-11), and have reported that DKK3 exerts oncogenic functions in HNSCC. Intriguingly, it has been demonstrated that DKK3 overexpression in HNSCC cells results in significantly increased cellular malignant properties *in vitro* and *in vivo* (11). To confirm the oncogenic roles of DKK3, a stable knockdown of DKK3 was generated and the effects of DKK3 loss-of-function were analyzed in HSC-3 cells. Compared with in our previous gain-of-function experiment, DKK3 knockdown resulted in decreased cellular proliferation, migration, invasion, and tumor cell growth and proliferation *in vivo*. In addition, microarray and pathway analyses suggested involvement of the PI3K/mTOR/Akt and MAPK pathways, thus indicating that DKK3 may modulate cancer cell malignant properties via the PI3K/mTOR/Akt and MAPK pathways.

A recent study regarding gene alterations and mutations suggested that the PI3K/Akt/mTOR and MAPK kinase-MAPK signaling pathways may be targeted in HNSCC (29). PI3K/Akt/mTOR signaling is a critical pathway for cell growth, survival and metabolism, and its functional activation is frequently detected in HNSCC cells and tissue samples (30-33). Activated PI3K results in activation of Akt via direct phosphorylation of Akt (Ser473) (34). Phosphatidylinositol (3,4,5)-trisphosphate may also indirectly activate Akt via recruiting PDK1 protein. Akt is a serine/threonine kinase that regulates numerous cellular responses, including cell proliferation, cell growth, protein synthesis and apoptosis. Activated Akt can activate mTORC1 and mTORC2, and promote cell growth and inhibition of apoptosis. The present data revealed that DKK3 knockdown decreased phosphorylation of Akt (Ser473), which was accompanied by decreased phosphorylation of PI3K (both p85 and p55) and PDK1. These findings indicated that DKK3 may modulate PI3K/Akt signaling both directly and indirectly. Generally, PI3K/Akt signaling is activated by stimulation from an activated receptor tyrosine kinase or G-protein coupled receptor. The present data suggested the existence of a specific cell membrane receptor for DKK3; however, no such receptor has been identified yet.

The present study explored another possible mechanism. Akt is also directly activated by mTORC2 (34). DEPTOR, which is a component of mTORC2, is an endogenous regulator that directly interacts with the mTOR signaling pathway; overexpression of DEPTOR downregulates the activity of mTORC1 and mTORC2 (35). The present data revealed that DEPTOR expression was increased in HSC-3 shDKK3 cells, and DKK3 overexpression in HSC-3 shDKK3 cells decreased DEPTOR expression.

Supporting the present data, the tumor suppressor role of DEPTOR has been reported in several malignancies, including squamous cell carcinoma (SCC). For example, Ji *et al* reported that DEPTOR functions as a tumor suppressor, which suppresses tumor cell growth of esophageal SCC, and downregulation of DEPTOR expression predicts a poor prognosis (36). Recently, Baldassarri *et al* reported that DEPTOR is under-expressed in normal and tumor tissues in non-smoking female patients with lung SCC (37). With regards to the mechanism underlying how DKK3 modulates Akt via mTOR, Gao *et al* reported that stability of DEPTOR is controlled by the β-transducin repeats-containing proteins (TrCP) E3 ubiquitin ligase, and that failure to degrade DEPTOR by degron mutation or β-TrCP depletion leads to reduced activity of mTOR (38). In addition, β-TrCP is known to interact with intracellular DKK3 to block nuclear translocation of β-catenin via β-catenin re-distribution (39,40). Taken together, DKK3 may interact with β-TrCP and degrade DEPTOR, thus resulting in mTORC2 activation and consequent Akt phosphorylation. Therefore, DKK3 knockdown may result in increased DEPTOR expression, and decreased phosphorylation of mTOR and Akt.

To highlight the possible AKT/PI3K activation in HNSCC and to confirm whether DKK3 serves oncogenic roles in other types of cancer, TCGA tissue database was used. The results demonstrated that high mRNA expression levels of DKK3 were an unfavorable prognostic marker for HNSCC, pancreatic cancer and renal cancer, despite previous reports suggesting the tumor suppressor role of DKK3. Conversely, high DKK3 mRNA expression was associated with a favorable prognosis in prostate cancer, which is concordant with a previous report (6), thus suggesting that DKK3 may possess tumor- or tissue-specific roles. Furthermore, high PIK3CA, Akt1 and β-catenin mRNA expression, and low DEPTOR mRNA expression, were associated with a poor prognosis.

Moreover, microarray and pathway analyses also suggested other possible mechanisms associated with DKK3 expression,

which may modulate the malignant potential of HNSCC cells. For example, CXCL8, also known as interleukin 8, is a chemokine secreted by macrophages, epithelial cells and endothelial cells, which functions as a neutrophil chemotactic factor. It has been reported that CXCL8 expression is high in HNSCC, contributing to cancer cell invasion (41), and that CXCL8 secreted by tumor-associated macrophages and cancer cells enhances cancer cell migration and invasion in esophageal SCC (42). In addition, high expression of Rho-associated protein kinase-1 is associated with lymph node metastasis in laryngeal SCC (43). Another important gene is hypoxia-inducible factor 1α, of which high expression may be associated with invasion of oral SCC (44). These alterations in the gene expression profile of DKK3 knockdown cells may also partially explain the decreased malignant potential of these cancer cells.

In conclusion, the present study was the first, to the best of our knowledge, to demonstrate the oncogenic function of DKK3, and to report the possible molecular mechanism by which DKK3 activates Akt in HNSCC cells. The results indicated that DKK3 may be considered a promising therapeutic target for the treatment of HNSCC.

Acknowledgements

Not applicable.

Funding

The present study was supported by a Grant-in-Aid for Young Scientists (B) (grant no. 25861742 to NK) and a Grant-in-Aid for Scientific Research (C) (grant no. 16K11470 to NK) from MEXT KAKENHI; Research Project grants from Kawasaki Medical School (grant nos. 25-S-3, 26-B-34 and 27-B-063 to NK), and grants from the KAWASAKI Foundation for Medical Science and Medical Welfare (grant no. 2013-06 to NK), the Wesco Scientific Promotion Foundation (grant no. 2016-39 to NK) and the Takeda Science Foundation (grant no. 2018047114 to NK).

Availability of data and materials

All data generated or analyzed during this study are included in this published article. The microarray data are available in the GEO (accession no. GSE107403; https://www.ncbi.nlm.nih.gov/geo/query/acc.cgi?acc=GSE107403).

Authors' contributions

NK conceived and designed the experiments, and prepared the paper. NK and SIN performed the experiments. NK, SIN, AY, MY and SF analyzed the data. SF revised the manuscript and figures, and approved the article. All authors read and approved the manuscript and agree to be accountable for all aspects of the research in ensuring that the accuracy or integrity of any part of the work are appropriately investigated and resolved.

Ethics approval and consent to participate

Animal studies were conducted according to the recommendations outlined in the Guidelines for Animal Experiments at Kawasaki Medical School. Animal experiments were approved by the Animal Care and Use Committee of Kawasaki Medical School.

Patient consent to publication

Not applicable.

Competing interests

The authors declare that they have no competing interests.

References

1. Sarode GS, Sarode SC, Maniyar N, Anand R and Patil S: Oral cancer databases: a comprehensive review. J Oral Pathol Med 47: 547-556, 2018.
2. Ali J, Sabiha B, Jan HU, Haider SA, Khan AA and Ali SS: Genetic etiology of oral cancer. Oral Oncol 70: 23-28, 2017.
3. Veeck J and Dahl E: Targeting the Wnt pathway in cancer: The emerging role of Dickkopf-3. Biochim Biophys Acta 1825: 18-28, 2012.
4. Tsuji T, Miyazaki M, Sakaguchi M, Inoue Y and Namba M: A REIC gene shows down-regulation in human immortalized cells and human tumor-derived cell lines. Biochem Biophys Res Commun 268: 20-24, 2000.
5. Katase N and Nohno T: DKK3 (dickkopf 3 homolog (*Xenopus laevis*)). Atlas Genet Cytogenet Oncol Haematol 17: 678-686, 2013.
6. Edamura K, Nasu Y, Takaishi M, Kobayashi T, Abarzua F, Sakaguchi M, Kashiwakura Y, Ebara S, Saika T, Watanabe M, *et al*: Adenovirus-mediated REIC/Dkk-3 gene transfer inhibits tumor growth and metastasis in an orthotopic prostate cancer model. Cancer Gene Ther 14: 765-772, 2007.
7. Kawasaki K, Watanabe M, Sakaguchi M, Ogasawara Y, Ochiai K, Nasu Y, Doihara H, Kashiwakura Y, Huh NH, Kumon H, *et al*: REIC/Dkk-3 overexpression downregulates P-glycoprotein in multidrug-resistant MCF7/ADR cells and induces apoptosis in breast cancer. Cancer Gene Ther 16: 65-72, 2009.
8. Fujii M, Katase N, Lefeuvre M, Gunduz M, Buery RR, Tamamura R, Tsujigiwa H and Nagatsuka H: Dickkopf (Dkk)-3 and β-catenin expressions increased in the transition from normal oral mucosal to oral squamous cell carcinoma. J Mol Histol 42: 499-504, 2011.
9. Katase N, Lefeuvre M, Gunduz M, Gunduz E, Beder LB, Grenman R, Fujii M, Tamamura R, Tsujigiwa H and Nagatsuka H: Absence of Dickkopf (Dkk)-3 protein expression is correlated with longer disease-free survival and lower incidence of metastasis in head and neck squamous cell carcinoma. Oncol Lett 3: 273-280, 2012.
10. Katase N, Lefeuvre M, Tsujigiwa H, Fujii M, Ito S, Tamamura R, Buery RR, Gunduz M and Nagatsuka H: Knockdown of Dkk-3 decreases cancer cell migration and invasion independently of the Wnt pathways in oral squamous cell carcinoma-derived cells. Oncol Rep 29: 1349-1355, 2013.
11. Katase N, Nishimatsu SI, Yamauchi A, Yamamura M, Terada K, Itadani M, Okada N, Hassan NMM, Nagatsuka H, Ikeda T, *et al*: DKK3 overexpression increases the malignant properties of head and neck squamous cell carcinoma cells. Oncol Res 26: 45-58, 2018.
12. de Jonge HJ, Fehrmann RS, de Bont ES, Hofstra RM, Gerbens F, Kamps WA, de Vries EG, van der Zee AG, te Meerman GJ and ter Elst A: Evidence based selection of housekeeping genes. PLoS One 2: e898, 2007.
13. Katase N, Terada K, Suzuki T, Nishimatsu S and Nohno T: miR-487b, miR-3963 and miR-6412 delay myogenic differentiation in mouse myoblast-derived C2C12 cells. BMC Cell Biol 16: 13, 2015.
14. Huang W, Sherman BT and Lempicki RA: Systematic and integrative analysis of large gene lists using DAVID bioinformatics resources. Nat Protoc 4: 44-57, 2009.
15. Huang W, Sherman BT and Lempicki RA: Bioinformatics enrichment tools: Paths toward the comprehensive functional analysis of large gene lists. Nucleic Acids Res 37: 1-13, 2009.

16. Gao J, Aksoy BA, Dogrusoz U, Dresdner G, Gross B, Sumer SO, Sun Y, Jacobsen A, Sinha R, Larsson E, *et al*: Integrative analysis of complex cancer genomics and clinical profiles using the cBioPortal. Sci Signal 6: pl1, 2013.
17. Cerami E, Gao J, Dogrusoz U, Gross BE, Sumer SO, Aksoy BA, Jacobsen A, Byrne CJ, Heuer ML, Larsson E, *et al*: The cBio cancer genomics portal: An open platform for exploring multidimensional cancer genomics data. Cancer Discov 2: 401-404, 2012.
18. Uhlen M, Zhang C, Lee S, Sjöstedt E, Fagerberg L, Bidkhori G, Benfeitas R, Arif M, Liu Z, Edfors F, *et al*: A pathology atlas of the human cancer transcriptome. Science 357: eaan2507, 2017.
19. Pickering CR, Zhang J, Yoo SY, Bengtsson L, Moorthy S, Neskey DM, Zhao M, Ortega Alves MV, Chang K, Drummond J, *et al*: Integrative genomic characterization of oral squamous cell carcinoma identifies frequent somatic drivers. Cancer Discov 3: 770-781, 2013.
20. Sharma V, Nandan A, Sharma AK, Singh H, Bharadwaj M, Sinha DN and Mehrotra R: Signature of genetic associations in oral cancer. Tumour Biol 39: 1010428317725923, 2017.
21. Khayer N, Zamanian-Azodi M, Mansouri V, Ghassemi-Broumand M, Rezaei-Tavirani M, Heidari MH and Rezaei Tavirani M: Oral squamous cell cancer protein-protein interaction network interpretation in comparison to esophageal adenocarcinoma. Gastroenterol Hepatol Bed Bench 10: 118-124, 2017.
22. Upadhyay P, Gardi N, Desai S, Chandrani P, Joshi A, Dharavath B, Arora P, Bal M, Nair S and Dutt A: Genomic characterization of tobacco/nut chewing HPV-negative early stage tongue tumors identify MMP10 asa candidate to predict metastases. Oral Oncol 73: 56-64, 2017.
23. Nayak S, Goel MM, Makker A, Bhatia V, Chandra S, Kumar S and Agarwal SP: Fibroblast growth factor (FGF-2) and its receptors FGFR-2 and FGFR-3 may be putative biomarkers of malignant transformation of potentially malignant oral lesions into oral squamous cell carcinoma. PLoS One 10: e0138801, 2015.
24. Chang KY, Tsai SY, Chen SH, Tsou HH, Yen CJ, Liu KJ, Fang HL, Wu HC, Chuang BF, Chou SW, *et al*: Dissecting the EGFR-PI3K-AKT pathway in oral cancer highlights the role of the EGFR variant III and its clinical relevance. J Biomed Sci 20: 43, 2013.
25. Katase N, Gunduz M, Beder L, Gunduz E, Lefeuvre M, Hatipoglu OF, Borkosky SS, Tamamura R, Tominaga S, Yamanaka N, *et al*: Deletion at Dickkopf (dkk)-3 locus (11p15.2) is related with lower lymph node metastasis and better prognosis in head and neck squamous cell carcinomas. Oncol Res 17: 273-282, 2008.
26. Katase N, Gunduz M, Beder LB, Gunduz E, Al Sheikh Ali M, Tamamura R, Yaykasli KO, Yamanaka N, Shimizu K and Nagatsuka H: Frequent allelic loss of Dkk-1 locus (10q11.2) is related with low distant metastasis and better prognosis in head and neck squamous cell carcinomas. Cancer Invest 28: 103-110, 2010.
27. Chen L, Wang K, Shao Y, Huang J, Li X, Shan J, Wu D and Zheng JJ: Structural insight into the mechanisms of Wnt signaling antagonism by Dkk. J Biol Chem 283: 23364-23370, 2008.
28. Fujii Y, Hoshino T and Kumon H: Molecular simulation analysis of the structure complex of C2 domains of DKK family members and β-propeller domains of LRP5/6: Explaining why DKK3 does not bind to LRP5/6. Acta Med Okayama 68: 63-78, 2014.
29. Van Waes C and Musbahi O: Genomics and advances towards precision medicine for head and neck squamous cell carcinoma. Laryngoscope Investig Otolaryngol 2: 310-319, 2017.
30. Wang SQ, Wang X, Zheng K, Liu KS, Wang SX and Xie CH: Simultaneous targeting PI3K and PERK pathways promotes cell death and improves the clinical prognosis in esophageal squamous carcinoma. Biochem Biophys Res Commun 493: 534-541, 2017.
31. Wang Z, Valera JC, Zhao X, Chen Q and Silvio Gutkind J: mTOR co-targeting strategies for head and neck cancer therapy. Cancer Metastasis Rev 36: 491-502, 2017.
32. Simpson DR, Mell LK and Cohen EE: Targeting the PI3K/AKT/mTOR pathway in squamous cell carcinoma of the head and neck. Oral Oncol 51: 291-298, 2015.
33. Li SH, Chien CY, Huang WT, Luo SD, Su YY, Tien WY, Lan YC and Chen CH: Prognostic significance and function of mammalian target of rapamycin in tongue squamous cell carcinoma. Sci Rep 7: 8178, 2017.
34. Rogers SJ, Box C, Harrington KJ, Nutting C, Rhys-Evans P and Eccles SA: The phosphoinositide 3-kinase signalling pathway as a therapeutic target in squamous cell carcinoma of the head and neck. Expert Opin Ther Targets 9: 769-790, 2005.
35. Peterson TR, Laplante M, Thoreen CC, Sancak Y, Kang SA, Kuehl WM, Gray NS and Sabatini DM: DEPTOR is an mTOR inhibitor frequently overexpressed in multiple myeloma cells and required for their survival. Cell 137: 873-886, 2009.
36. Ji YM, Zhou XF, Zhang J, Zheng X, Li SB, Wei ZQ, Liu T, Cheng DL, Liu P, Song K, *et al*: DEPTOR suppresses the progression of esophageal squamous cell carcinoma and predicts poor prognosis. Oncotarget 7: 14188-14198, 2016.
37. Baldassarri M, Fallerini C, Cetta F, Ghisalberti M, Bellan C, Furini S, Spiga O, Crispino S, Gotti G, Ariani F, *et al*: Omic approach in non-smoker female with lung squamous cell carcinoma pinpoints to germline susceptibility and personalized medicine. Cancer Res Treat 50: 356-365, 2018.
38. Gao D, Inuzuka H, Tan MK, Fukushima H, Locasale JW, Liu P, Wan L, Zhai B, Chin YR, Shaik S, *et al*: mTOR drives its own activation via SCF(βTrCP)-dependent degradation of the mTOR inhibitor DEPTOR. Mol Cell 44: 290-303, 2011.
39. Lee EJ, Jo M, Rho SB, Park K, Yoo YN, Park J, Chae M, Zhang W and Lee JH: Dkk3, downregulated in cervical cancer, functions as a negative regulator of beta-catenin. Int J Cancer 124: 287-297, 2009.
40. Leonard JL, Leonard DM, Wolfe SA, Liu J, Rivera J, Yang M, Leonard RT, Johnson JPS, Kumar P, Liebmann KL, *et al*: The Dkk3 gene encodes a vital intracellular regulator of cell proliferation. PLoS One 12: e0181724, 2017.
41. Warner KA, Miyazawa M, Cordeiro MM, Love WJ, Pinsky MS, Neiva KG, Spalding AC and Nör JE: Endothelial cells enhance tumor cell invasion through a crosstalk mediated by CXC chemokine signaling. Neoplasia 10: 131-139, 2008.
42. Hosono M, Koma YI, Takase N, Urakawa N, Higashino N, Suemune K, Kodaira H, Nishio M, Shigeoka M, Kakeji Y, *et al*: CXCL8 derived from tumor-associated macrophages and esophageal squamous cell carcinomas contributes to tumor progression by promoting migration and invasion of cancer cells. Oncotarget 8: 106071-106088, 2017.
43. Zhang J, He X, Ma Y, Liu Y, Shi H, Guo W and Liu L: Overexpression of ROCK1 and ROCK2 inhibits human laryngeal squamous cell carcinoma. Int J Clin Exp Pathol 8: 244-251, 2015.
44. Lin PY, Yu CH, Wang JT, Chen HH, Cheng SJ, Kuo MY and Chiang CP: Expression of hypoxia-inducible factor-1 alpha is significantly associated with the progression and prognosis of oral squamous cell carcinomas in Taiwan. J Oral Pathol Med 37: 18-25, 2008.